

Average dynamics of a driven set of globally coupled excitable units

Leandro M. Alonso and Gabriel B. Mindlin

Department of Physics, FCEyN, UBA, Ciudad Universitaria, Pab I, cp 1428, Buenos Aires, Argentina

(Received 20 December 2010; accepted 14 March 2011; published online 7 April 2011)

We investigate the behavior of the order parameter describing the collective dynamics of a large set of driven, globally coupled excitable units. We derive conditions on the parameters of the system that allow to bound the degree of synchrony of its solutions. We describe a regime where time dependent nonsynchronous dynamics occurs and, yet, the average activity displays low dimensional, temporally complex behavior. © 2011 American Institute of Physics. [doi:10.1063/1.3574030]

The study of the collective dynamics of a noncompletely synchronized extended system started with the work of Kuramoto,¹ who showed that a large set of sinusoidally coupled phase oscillators could display a collective state consisting of a mixture of synchronized and non-synchronized units. The average dynamics of such state would be a stationary rotation of a magnitude depending on the strength of the coupling between the units and the dispersion of their individual frequencies. Recently, Ott and Antonsen^{2,3} found that the model by Kuramoto presents an invariant manifold, i.e., a set of states for which the macroscopic dynamics becomes low dimensional. This strategy was later applied to solve closely related problems, as the dynamics of a set of periodically forced coupled oscillators.⁴ In this work, we investigate the behavior of an order parameter that describes the collective dynamics of a large set of driven, globally excitable units. We find that low dimensional and yet complex dynamics can be found in the average activity of the array, in a regime presenting a time dependent degree of synchrony.

In this work, we are interested in exploring the dynamics of a forced set of globally coupled excitable systems. The dynamics of each unit, before coupling, is ruled by

$$\dot{\theta} = \omega - \gamma \sin(\theta). \quad (1)$$

If $\omega/\gamma < 1$, the system has two fixed points, one stable and the other unstable. The separation between these fixed points depends on the ω/γ ratio. The qualitative behavior of this system is shown in Fig. 1, where we display the response of the system to different initial conditions. If these are close to the quiescent state, the system rapidly decays to the stable fixed point. For initial conditions above some threshold, the response of the system includes a large excursion in the phase space before decaying to the stable fixed point.

In our study, the forcing units will be represented mathematically by phase oscillators. We assume that there is a global coupling between all driven excitable units, a global coupling between all forcing units, and a directed coupling from the driving units to the network of excitable, driven units. Following Ott and Antonsen, we derive equations describing the average dynamics of the system under study in a low dimensional invariant manifold. We will show that low dimensional and yet non trivial dynamics is possible at the macroscopic level. We identify regions of the parameter space for which the dynamics of the order parameter is unbounded, therefore yielding low dimensional, nontrivial dynamics. We support our conclusions with numerical simulations of the extended system.

I. INTRODUCTION

The study of the generic features presented by a large number of coupled oscillators has a long history.⁵ In part, this is due to the wide range of areas where this problem emerges. Kuramoto made a seminal contribution to the field by introducing a mathematical model that allowed some analytic treatment. The dynamics of each oscillator was described in terms of its phase, and the coupling between the different oscillators was assumed to be sinusoidal, yielding a simplification of the analysis of the model. By introducing a mean field function, he obtained an indicator of the coherence of the units. He found that the oscillators are forced by the mean field and, depending on their parameters, they can synchronize with it. Recently, Ott and Antonsen^{2,3} found that the model by Kuramoto presents an invariant manifold, i.e., a set of states, for which the macroscopic dynamics becomes low dimensional.

II. THE MODEL

Our model consists of two sets of phase oscillators. Set 1 refers to the driving set, while set 2 refers to the driven set. We use Greek letters to indicate population number and Latin letters to index the elements within a population. Using this notation, we have the full extended model:

$$\dot{\theta}_i^\sigma = \omega_i^\sigma - \gamma_i^\sigma \sin(\theta_i^\sigma) + \sum_{\sigma'=1}^2 \frac{K_{\sigma\sigma'}}{N^{\sigma'}} \sum_{j=1}^{N^{\sigma'}} \sin(\theta_j^{\sigma'} - \theta_i^\sigma), \quad (2)$$

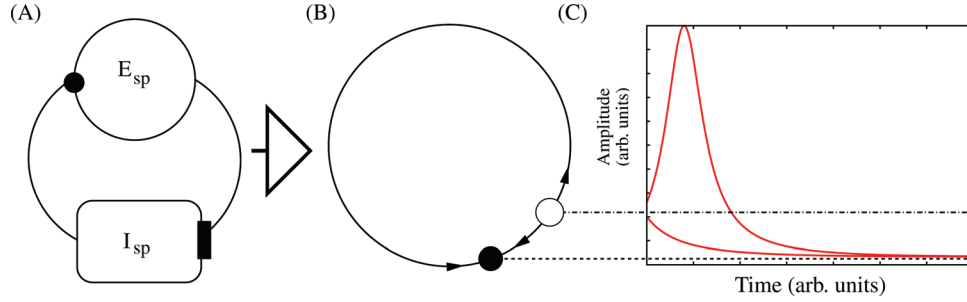


FIG. 1. (Color online) (a) Schematics of a neural oscillator. The circle on the top represents an excitatory subpopulation of neurons (E_{sp}), while the rectangle represents the inhibitory one (I_{sp}). (b) Mathematical representation of the neural oscillator by a phase oscillator. The main dynamical features of the neural oscillator close to a $SNLC \ll$ bifurcation are captured by this simple model. (c) Qualitative behavior of the phase oscillator model. For initial conditions below the threshold (indicated by the dashed line), the solution is a rapid decay to the stable fixed point, while for initial conditions above this threshold, the system performs a large excursion in phase space. This means that small perturbations from the stable fixed point will result in rapid decay to equilibrium. For perturbations that are large enough, the system response is qualitatively different. Adapted from Ref. 12.

where, for each population, the natural frequency of the i th oscillator is denoted by ω_i^σ . The parameter ruling the excitable nature of each unit is γ_i^σ , the number of oscillators in the population is given by N^σ , and $K_{\sigma\sigma'}$ stands for the connectivity matrix.

In the limit $N^\sigma \rightarrow \infty$, these populations can be described in terms of density probability functions $f^\sigma(\theta, \omega, t)$, with $\sigma = 1, 2$. The evolution of f^σ is given by the continuity equation,

$$\frac{\partial f^\sigma}{\partial t} + \frac{\partial}{\partial \theta}(f^\sigma v^\sigma) = 0, \quad (3)$$

where the velocity v is given by:

$$v^\sigma(\theta^\sigma, \omega, t) = \omega^\sigma - \gamma^\sigma \sin(\theta^\sigma) + \sum_{\sigma'=1}^2 K_{\sigma\sigma'} \times \int_{-\infty}^{\infty} \int_0^{2\pi} \sin(\theta' - \theta^\sigma) f^{\sigma'}(\theta', \omega, t) d\theta' d\omega. \quad (4)$$

We have defined f^σ in such a way that the fraction of oscillators with phases between θ and $\theta + d\theta$ and natural frequencies between ω and $\omega + d\omega$ is given by $f^\sigma(\theta, \omega, t) d\theta d\omega$. Therefore, in order to close the system, we need that the following equations are satisfied:

$$\left\{ \begin{array}{l} \int_{-\infty}^{\infty} \int_0^{2\pi} f^\sigma(\theta, \omega, t) d\theta d\omega = 1 \\ \int_0^{2\pi} f^\sigma(\theta, \omega, t) d\theta = g^\sigma(\omega) \end{array} \right\}. \quad (5)$$

As suggested by Kuramoto, we define the system complex order parameter as

$$r^\sigma(t) = \sum_{\sigma'=1}^2 K_{\sigma\sigma'} z^{\sigma'}, \quad (6)$$

where z^σ is the complex average of the oscillators in σ th population given by the following equation:

$$z^\sigma = \int_{-\infty}^{\infty} \int_0^{2\pi} e^{i\theta} f^\sigma(\theta, \omega, t) d\theta d\omega. \quad (7)$$

With these definitions, the velocity (4) simplifies to

$$v^\sigma(\theta^\sigma, \omega, t) = \omega^\sigma + \frac{\gamma^\sigma}{2i} (e^{i\theta^\sigma} - e^{-i\theta^\sigma}) + \frac{1}{2i} (e^{-i\theta^\sigma} r^{\sigma} - e^{i\theta^\sigma} r^{\sigma*}), \quad (8)$$

where the super index $*$ denotes the complex conjugation. We are interested in the case of a population of phase oscillators driving a population of excitable units. We accomplish this by making $\gamma^{\sigma=1} = 0$ and $K_{12} = 0$. In this way, we reduce this population to one behaving as in the case described by Kuramoto. We simplify the notation and leave $\gamma^{\sigma=2} = \gamma$ as a parameter of the model.

It is a conventional strategy to address this problem by expanding f^σ in a Fourier series in θ ,

$$f^\sigma(\theta^\sigma, \omega, t) = \frac{g(\omega)}{2\pi} \left[1 + \sum_{n=1}^{\infty} f_n^\sigma(\omega, t) e^{in\theta^\sigma} + cc \right], \quad (9)$$

with cc denoting complex conjugation. Replacing (9) and (8) into (3), one obtains, in principle, an infinite dimensional system of equations for f_n^σ .

An important breakthrough in the analysis of this problem was reported by Antonsen and Ott,² who noticed that the following ansatz $f_n^\sigma(\omega, t) = (\alpha_\sigma(\omega, t))^n$ would satisfy all the amplitude equations as long as certain equations are satisfied by α_σ . For our problem, these read as follows:

$$\left\{ \begin{array}{l} \dot{\alpha}_1 = -i\omega\alpha_1 + \frac{K_{11}}{2} (\alpha_1 - |\alpha_1|^2 \alpha_1) \\ \dot{\alpha}_2 = -i\omega\alpha_2 + \frac{\gamma}{2} (1 - \alpha_2^2) + \frac{K_{22}}{2} (\alpha_2 - |\alpha_2|^2 \alpha_2) + \frac{K_{21}}{2} (\alpha_1 - \alpha_1^* \alpha_2^2) \end{array} \right\}. \quad (10)$$

By further assuming that $g^\sigma(\omega)$ is a Lorentzian,

$$g^\sigma(\omega) = \frac{\Delta^\sigma}{\pi [(\omega - \omega_0^\sigma)^2 + (\Delta^\sigma)^2]}, \quad (11)$$

and that $\alpha_\sigma(\omega, t)$ satisfies certain analyticity conditions in the complex ω -plane, Ott and Antonsen² evaluated Eq. (10) by contour integration. By multiplying both sides of (10) by $g^\sigma(\omega)$ and using the residue theorem, we have the following equations for the evolution of $\alpha_\sigma(\omega_0^\sigma - i\Delta^\sigma, t)$:

$$\left\{ \begin{aligned} \alpha_1(\omega_0^1 - i\Delta^1, t) &= -i(\omega_0^1 - i\Delta^1)\alpha_1 + \frac{K_{11}}{2}(\alpha_1 - |\alpha_1|^2\alpha_1) \\ \alpha_2(\omega_0^2 - i\Delta^2, t) &= -i(\omega_0^2 - i\Delta^2)\alpha_2 + \frac{\gamma}{2}(1 - \alpha_2^2) + \frac{K_{22}}{2}(\alpha_2 - \alpha_2^2\alpha_2) + \frac{K_{21}}{2}(\alpha_1 - \alpha_1^*\alpha_2^*) \end{aligned} \right\}, \quad (12)$$

where the arguments of $\alpha_\sigma(\omega_0^\sigma - i\Delta^\sigma, t)$ were dropped for notational simplicity in the right-hand sides. By using the Fourier expansion (9) of the distribution function and the ansatz in (7), we have the relation between the distribution function and the order parameters for each set of units:

$$\begin{aligned} z^\sigma(t) &= \int_{-\infty}^{\infty} \int_0^{2\pi} e^{i\theta} f^\sigma(\theta, \omega, t) d\theta d\omega \\ &= \int_{-\infty}^{\infty} \alpha_\sigma^* g(\omega) d\omega = \alpha_\sigma^*(\omega_0^\sigma - i\Delta^\sigma, t). \end{aligned} \quad (13)$$

We can write the order parameter in its Euler form as $z^\sigma(t) = \rho^\sigma(t)e^{i\theta^\sigma(t)}$. The average phase position of the oscillators is given by $\theta^\sigma(t)$ while the modulus $\rho^\sigma(t)$ measures how peaked its distribution is.

tors is given by $\theta^\sigma(t)$ while the modulus $\rho^\sigma(t)$ measures how peaked its distribution is.

III. MAIN RESULTS

The driving population ($\sigma = 1$), as discussed by Kuramoto, presents a collective state, which can be described by an order parameter $\alpha_1 = \sqrt{1 - 2\Delta^1/K_{11}} = \rho_1$, and a phase ϕ_1 rotating at ω_0^1 . The second population, on the other hand, can be described in terms of the modulus and phase of α_2 , thus yielding a three-dimensional system of differential equations:

$$\left\{ \begin{aligned} \dot{\rho}_2 &= -\Delta_0^2 \rho_2 + \frac{\gamma}{2} \cos(\phi_2)(1 - \rho_2^2) + \frac{K_{22}}{2} \rho_2(1 - \rho_2^2) + \frac{K_{21}}{2} \rho_1 \cos(\phi_1 - \phi_2)(1 - \rho_2^2) \\ \dot{\phi}_2 &= -\omega_0^2 - \frac{\gamma}{2} \sin(\phi_2) \left(\rho_2 + \frac{1}{\rho_2} \right) + K_{21} \frac{\rho_1}{\rho_2} \sin(\phi_1 - \phi_2)(1 + \rho_2^2) \\ \dot{\phi}_1 &= -\omega_0^1 \end{aligned} \right\}, \quad (14)$$

where Δ_0^i and Ω_0^i are the width and center of the assumed Lorentzian distribution of frequencies for the σ th population, respectively. In the limit $\Delta_0^2 \rightarrow 0$, $\rho = 1$ is the solution, and therefore the system presents a dynamics constrained to a torus. Notice that for $\Delta_0^2 > 0$, the system is fully three-dimensional, and in principle, the average activity of the driven population can present low dimensional chaos. It is worth remarking that the low dimensional chaos in the average activity of the driven population cannot be found without time dependent asynchrony.

There are two different regions of the parameter space where the dynamics is qualitatively different. Notice that it is always possible to find values of ρ_2 such that $\dot{\rho}_2|_{\rho_2} < 0$, as long as

$$f(\rho_2) = \frac{\rho_2}{1 - \rho_2^2} > \frac{K_{22}}{2\Delta_0^2} \rho_2 + \frac{\gamma + K_{21}\rho_1}{2\Delta_0^2} = f_2(\rho_2). \quad (15)$$

It is also possible to look for values of ρ_2 such that $\dot{\rho}_2|_{\rho_2} > 0$. The condition that such values need to satisfy can be found to be

$$f(\rho_2) = \frac{\rho_2}{1 - \rho_2^2} < \frac{K_{22}}{2\Delta_0^2} \rho_2 - \frac{\gamma + K_{21}\rho_1}{2\Delta_0^2} = f_3(\rho_2). \quad (16)$$

Whenever both conditions can be satisfied simultaneously, the order parameter varies within boundaries: one can define a $\rho = \rho_{max}$ (ρ_{min}) as the lower (upper) boundary of the values over which $\dot{\rho} < 0$ (> 0). In this way, although the driven population is not fully synchronized, the order parameter is bounded from below. In Fig. 2, we use points to show the region of the parameter space $a = K_{22}/2\Delta_0^2$, $b = \gamma + K_{21}\rho_1/2\Delta_0^2$ where the system's order parameter has bounded dynamics

In Fig. 3, we display $f(\rho)$, $f_2(\rho)$, and $f_3(\rho)$ for the case where the order parameter is bounded and unbounded from below. If the slope of the straight lines ($f_{2,3}$) is smaller than a threshold value, there is no lower boundary for the order parameter. Since the slope is proportional to the coupling within the driven population, we infer that there is a minimum value of the global coupling such that a lower bound for the level of synchrony exists.

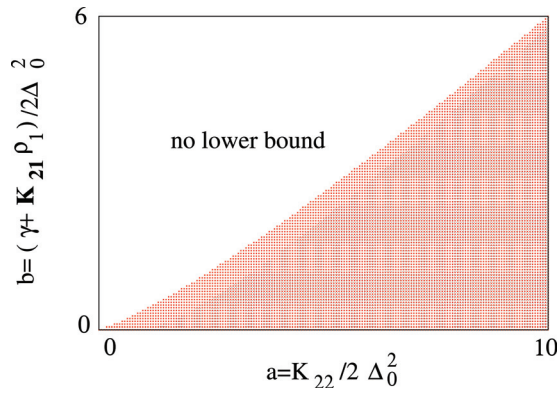


FIG. 2. (Color online) The regions of the parameter space where the system presents an order parameter bounded from below (dots). The parameters are $a = K_{22}/2\Delta_0^2$ and $b = (\gamma + K_{21}\rho_1)/2\Delta_0^2$. In our simulations, $\Delta_0^2 = 1$. The order parameter of the driving population was computed as $\rho_1 = \sqrt{1 - 2\Delta_0^1/K_{11}}$, with $\Delta_0^1 = 0.01$ and $K_{11} = 5.5$.

The order parameter fails to have a lower boundary if, for a given level of global coupling K_{22} , the system presents large values of γ , K_{21} , or ρ_1 . For each set of values used in Fig. 3(a), we performed a simulation with 100 excitable units forced by a set of other 100 phase oscillators. For each simulation, we computed $\langle \cos(\theta_i^2) \rangle$ and $\langle \sin(\theta_i^2) \rangle$, where $\langle \rangle$

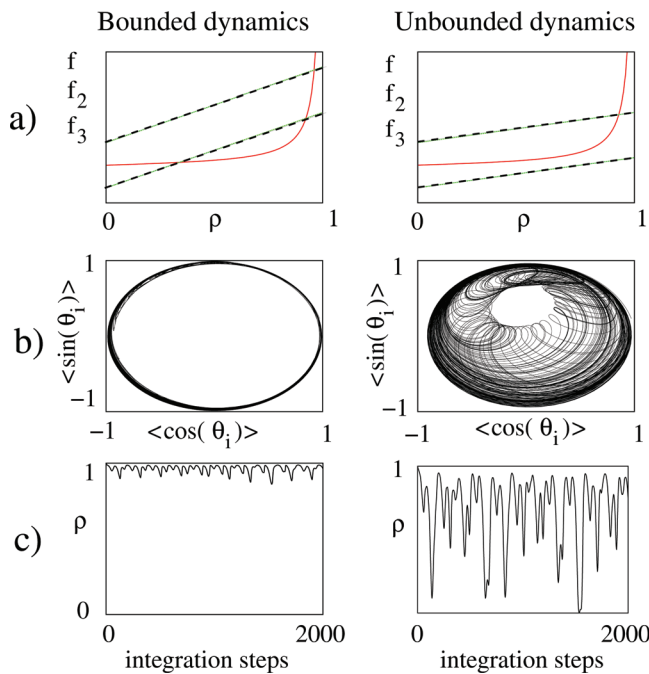


FIG. 3. (Color online) Boundaries for the order parameter of the driven population of units. In the left panels, the parameters are chosen so that there is a lower boundary for the order parameter of the extended system, which, therefore, preserves a degree of synchrony during its evolution. In the right panels, the parameters are chosen so that there is only an upper boundary for the order parameter. The conditions in the text [Eqs. (4) and (5)] are displayed geometrically in (a). We used continuous line for f and dashed line for f_2 and f_3 . Numerical simulations of the extended system, with 100 phase oscillators driving 100 excitable units are performed. The average values over the populations $\langle \cos(\theta_i) \rangle$ and $\langle \sin(\theta_i) \rangle$ are displayed in (b), while the time evolution of the order parameter is shown, for each choice of parameters, in the left and right panels of (c). In these simulations, $K_{21} = 6$, $\gamma = 4$, $\omega_0^1 = -10$, and $\omega_0^2 = 3.8$. The parameter $K_{22} = 20$ for the simulations on the left, while $K_{22} = 8$ for the simulations on the right.

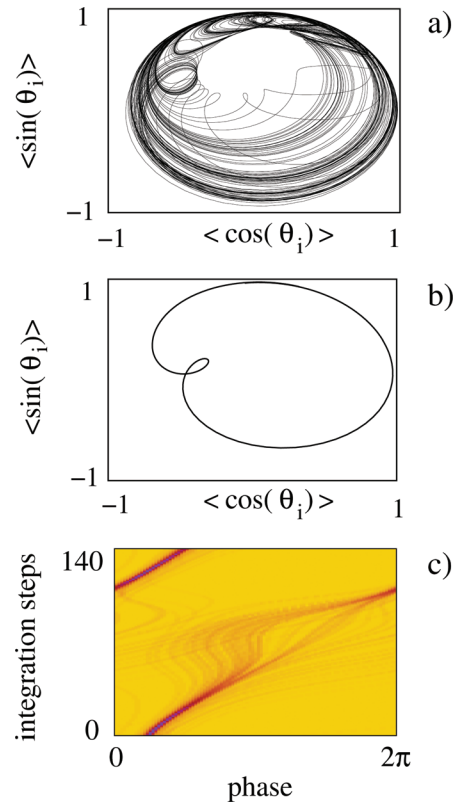


FIG. 4. (Color online) For the parameter values such that the averaged system displays chaotic dynamics, a simulation with one hundred oscillators. In (a), $\langle \cos(\theta_i) \rangle$ and $\langle \sin(\theta_i) \rangle$ are displayed. A close return analysis allows to reconstruct unstable periodic orbits coexisting with the attractor. One of such orbits is displayed in (b). The order parameter approaches zero when this orbit is visited. In (c), we display the histograms for different values of t , where the number of excitable driven units with phase between $(\theta, \theta + 2\pi/100)$ is color coded. For the periodic orbit to achieve its topological shape, the system has to temporarily lose synchrony. In these simulations, $K_{11} = 5.5$, $\gamma = 6.83$, $\omega_0^1 = 10$, $\omega_0^2 = 5.8$, $K_{22} = 10$, and $K_{21} = 5$.

stands for the average over the population. In Fig. 3(b), we show the results for the case of order parameter bounded (unbounded) from below. The time evolution of the order parameters corresponding to each case are displayed in Fig. 3(c) right and left, respectively. Notice that for the size of the accessible band of ρ_2 values to vanish, b has to go to zero. That requires both that γ and the product $K_{21}\rho_1$ tend to zero, i.e., recovering the configuration studied by Kuramoto.

In Fig. 4, we display the average activity of 100 oscillators⁶ for parameter values such that the averaged system presents chaotic dynamics, with order parameter unbounded from below (a). Notice that a fluctuating order parameter is necessary for the dynamics to depart from simple quasiperiodic behavior. In other words, chaotic average dynamics requires time dependent levels of synchronization. If the attractor of the extended system is chaotic, we expect a single trajectory to coexist with infinitely many unstable periodic orbits. The method of close returns⁷ allows to find pieces of the data set that resemble periodic orbits. We look for a time interval for which the system is close to an unstable periodic orbit (b) such that the order parameter decreases to almost zero. We compute a histogram counting how many oscillators present a phase within $(\theta, \theta + 2\pi/100)$ at each time t (c). Notice that when the order parameter approaches

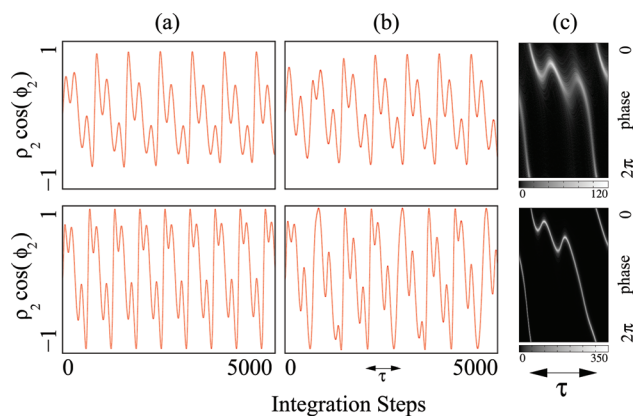


FIG. 5. (Color online) Top panels: (a) Numerical simulation of Eq. (14) showing a period 3 solution. The parameter values are $\rho_1 = \sqrt{1 - 2(0.01/8)}$ (thus, $K_{11} = 8$ and $\Delta^1 = 0.01$), $\omega_0^1 = 5$, $\omega^2 = 2.9$, $\gamma^2 = 2.96$, $\Delta^2 = 1$, $K_{21} = 2$, and $K_{22} = 8$. These parameters correspond to the unbounded region in Fig. 1. (b) Numerical simulation of the extended system 2. We used $N^1 = 100$ oscillators to drive $N^2 = 3000$ excitable oscillators. The frequencies ω_i^j were taken randomly from a Lorentzian distribution with mean $\omega_1 = 5$ ($\omega_2 = 2.9$) and deviation $\Delta_1 = 0.01$ ($\Delta_2 = 1$). The rest of the parameters are the same as in (a). (c) The histogram of population 2 for the temporal interval depicted by τ . The number of units with phase between $(\theta, \theta + (2\pi/500))$ is color coded. Bottom panels: (a) Numerical simulation of Eq. (14) showing a period 3 solution. The parameter values of the forcing are $\omega_0^1 = 6.4$ and $K_{21} = 2.6$. We chose $K_{22} = 20$ in order to be in the bounded region of Fig. 2. The rest of the parameters were left unchanged. The period 3 solution has the same topological features as in (a) top panel. In (b), we show the numerical simulation of the extended system. The parameters were chosen to agree with the previous simulation in the same way as in (b) top panel. The histogram evolution for the interval τ is shown in (c). The oscillators are in a highly synchronous state; however, the average behavior is similar to the top case. Thus, we show low dimensional nontrivial behavior emerging through qualitatively different mechanisms.

zero, the oscillators disperse: different oscillators are found in different phases. The system, therefore, behaves with a high degree of synchrony for some time, desynchronizes for a while, in such a way that the average activity of the population displays very well structured chaotic dynamics.

Low dimensional dynamics could emerge from an extended system as the result of a core of units locked subharmonically to a forcing, coexisting with asynchronous units whose average dynamics does not contribute to the average activity of the system. In Fig. 5, we show two period 3 solutions of Eq. (14), and its comparison to the extended system of Eq. (2). The parameters were chosen such that the solutions present the same topological features, but from regions of the parameter space that lead to unbounded and bounded dynamics, respectively. In this way, similar average dynamics was obtained through qualitatively different mechanisms. This alternative would not have existed for a chaotic solution that requires three dimensions and therefore time dependent asynchrony, as we have discussed.

It is worth to mention that the parameters of the system were chosen using the Arnold tongues diagram of system 14, i.e., the $N \rightarrow \infty$ limit. The agreement between the numerical simulations and the $N \rightarrow \infty$ theory is remarkable, particularly for the parameters where the dynamics is unbounded. For these cases, N as small as hundred units allowed us to obtain a good correspondence between the simulations of the extended system and the low dimensional system ruling the average activity.

IV. DISCUSSION AND CONCLUSIONS

How to obtain a macroscopic description of the dynamics presented by coupled nonlinear units is a problem with a long history in nonlinear dynamics. The seminal work of Kuramoto¹ on globally coupled oscillators opened a fruitful line of research. Recent advances²⁻⁴ allowed to explore closely related problems.

In this work, we studied the dynamics of a driven set of globally coupled excitable units. There are many systems that can be quoted as a motivation for this study. Coupled populations of excitatory and inhibitory neurons, for example, constitute an array that presents excitable dynamics⁸ for wide regions of its parameter space. Recently, arrays of this kind subjected to periodic forcing were conjectured to be related to the origin of physiological motor instructions used in birdsong production.⁹

The qualitatively different solutions that a low dimensional nonlinear system might present for different parameters has been proposed as a mechanism for obtaining nontrivial, yet robust motor patterns in biological systems.⁹⁻¹² These solutions would allow to having both robustness due to the low dimensionality as well as diversity. The possibility of reducing the dynamics of large sets of coupled oscillators or excitable units to an invariant manifold opens a new perspective to the study of those problems.

In our system, we show that nontrivial, low dimensional dynamics can be obtained as the average of forced, globally coupled excitable units. This behavior occurs without the need of a core of synchronized units, being the low dimensional dynamics the emergent of the average activity. Moreover, in the studied problem, some solutions cannot occur without time dependent levels of asynchrony; chaotic solutions are among them. This mechanism for generating chaotic dynamics is different from the one that involves the nonlinear interaction of a low number of spatial modes¹³ and constitutes an example of the rich dynamics that emerges from a large set of interacting nonlinear units.

¹Y. Kuramoto, *Self-Entrainment of a Population of Coupled Nonlinear Oscillators, Lecture Notes in Physics* (Springer, New York, 1975), Vol. 39, pp. 420–422.

²E. Ott and T. M. Antonsen, *Chaos* **18**, 037113 (2008).

³E. Ott and T. M. Antonsen, *Chaos* **19**, 023117 (2009).

⁴L. M. Childs and S. H. Strogatz, *Chaos* **18**, 043128 (2008).

⁵A. Pikovsky, M. Rosenblum, and J. Kurths, *Synchronization: A Universal Concept in Nonlinear Science* (Cambridge University Press, Cambridge, 2001).

⁶Although the results by Ott and Antonsen are strictly valid for $N \rightarrow \infty$, the average dynamics of a few hundred oscillators was well captured by the order parameters obeying 12.

⁷R. Gilmore and M. Lefranc, *The Topology of Chaos* (Wiley, Hoboken, 2002).

⁸F. C. Hoppensteadt and E. M. Izhikevich, *Weakly Connected Neural Networks*, (Springer-Verlag, New York, 1997).

⁹L. M. Alonso, J. A. Allende, and G. B. Mindlin, *Eur. J. Phys. D* **60**, 361 (2010).

¹⁰M. S. Golubitsky, I. Stewart, P.-L. Buono and J. J. Collins, *Nature (London)* **410**, 693 (1999).

¹¹M. A. Trevisan, G. B. Mindlin, and F. Goller, *Phys. Rev. Lett.* **96**, 058103 (2006).

¹²L. M. Alonso, J. A. Allende, F. Goller, and G. B. Mindlin, *Phys. Rev. E* **79**, 041929 (2009).

¹³E. N. Lorenz, *J. Atmos. Sci.* **20**, 130 (1963).